

Domain Walls, Wall Mobility, Coercivity and Initial
Permeability of **Metglas Fe₄₀Ni₃₈Mo₄B₁₈**

S. U. Jen (任盛源)

Institute of Physics, Academia Sinica, Taipei, Taiwan

(Received 26 December, 1986)

A multi-purpose Kerr-microscope system is set up for domain observations in static or dynamic cases. The material under investigation is Metglas Fe₄₀Ni₃₈Mo₄B₁₈. After field annealing, stripe domains are found with the easy axis parallel to the induced field. We have performed the pulse field experiments to find wall mobility, intrinsic damping and Gilbert damping constants. The coercivity and permeability of the same material have also been measured at various frequencies and field amplitudes. From the discovered d.c. coercivity and initial permeability, we proposed a pinning wells model to explain the relation between the two quantities.

I. INTRODUCTION

Magnetic domains are known to exist in Ferro- or Ferri-magnetic materials. Essentially, all the phenomena associated with magnetic properties, such as coercivity, permeability, magnetoresistance, etc. are closely related to domains^{1,2}. Therefore, domain properties, either static or dynamic, are always the prime subject in ferromagnetism. In the past, because people were deeply involved in bubble memories, wall dynamics has been fully developed and studied^{3,4}. Recently, the intense interest of Magneto-optical recording also utilize the technique of domain observations^{5,6} and its related properties.

In this paper, it is not intended to discuss the technological aspects of domain applications. Instead, we focus our attention on the physics of domain walls. Particularly, these involve direct observations of static domains and studies of wall dynamics with our newly developed Kerr-microscope system and a proposed bulk-pinning well model to explain the inter-relation between coercivity and initial permeability of most ferro-magnetic materials. We have chosen Metglas 2826MB as a material to study, because it is magnetically soft⁷. That means we do not need very high fields to move the walls or to magnetize the sample. Additionally, the visibility of domains in this material was found to be reasonably good.

II. DOMAINS AND WALL DYNAMICS

The Metglas 2826MB ribbon was fabricated by Mr. D. R. Huang of Chung-Shan Institute⁸. The as-cast ribbon is about 2cm wide and $50\mu\text{m}$ thick. In order to observe domains, we must first polish at least one side of the ribbon. The polishing procedures are standard with $3\mu\text{m}$, $1\mu\text{m}$ and $0.05\mu\text{m}$ abrasives. A well-polished sample is about $40\mu\text{m}$ thick and looks shiny. Then, to achieve optimum magnetic properties, such as low coercivity H_c and well-defined stripe domains⁹, field-annealing is needed. We cut a piece of polished sample of 2mm wide and 3cm long and put it in a quartz tube for annealing. An anneal is performed at 350°C for one hour in a vacuum 10^{-6} Torr. At the end of the one hour, an axial magnetic field, supplied by the solenoid coils around the tube, is switched on. The cooling rate is about $1.2^\circ\text{C}/\text{min}$. The magnetic field is directed along the length of the sample so that an easy axis of that direction can be induced.

For domain observations, a Kerr-microscope system, as shown in Fig. 1 (a), is set up for this purpose. A 200W high-pressure mercury arc is used as a light source. Two Glan-Thompson prisms of high quality (with extinction ratio of 1×10^{-6}) are used as a polarizer and analyzer respectively. The angle of incidence is chosen to be 60° . For the best Kerr

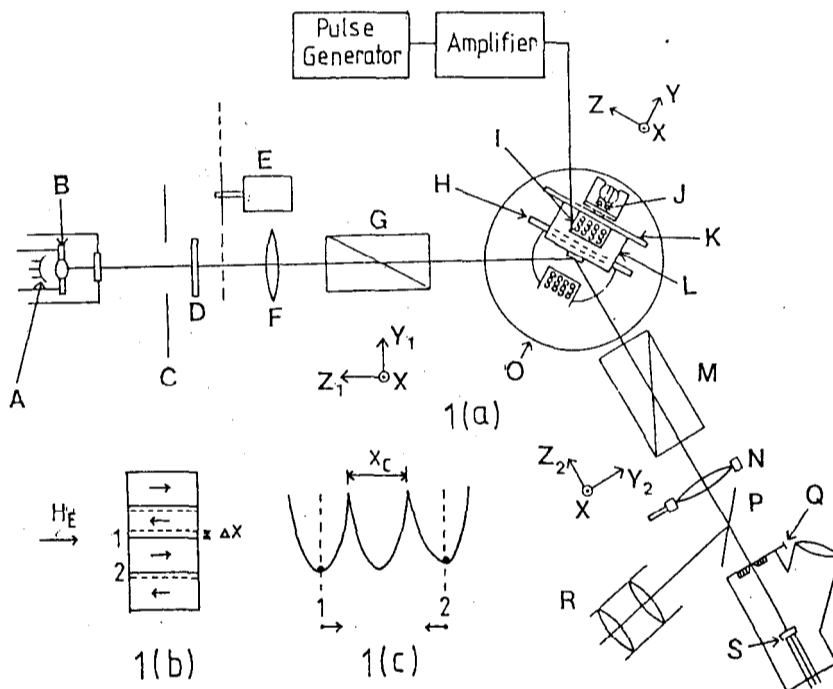


FIG. 1 (a) Kerr-microscope system. A & B: light Source, C: aperture, D: filter, E: shutters, F: condenser, G & M: Glan-Thompson prisms, H: cooling line, I: Helmholtz coils, J: set screw, K: back plate, L: sample holder, N: objective, P: mirror, Q: slit, R: eyepiece, S: photomultiplier.

1(b) Stripe domains under the action of a pulse, dc or ac field, Δx is the wall displacement.

1(c) Parabolic bulk pinning wells. Wall 1 and Wall 2 are at the bottom of each well, in equilibrium.

X_c is the size of the well.

contrast, we have used P-polarized light. The sample is mounted on a stage of the sample holder labeled L in Fig. 1(a). This stage can be rotated around the Y-axis. A Water-cooled Helmholtz coils are also equipped to give an external field of at least 20 mT. This field is large enough to saturate the sample in either the transverse or longitudinal directions. To work this Kerr-microscope, optical alignment is essential and the two prisms must close to extinction. Then, two or three domain walls are observed, parallel to the easy axis induced by the magnetic anneal. Because the domain contrast is weak, we only made visual observations, instead of using photography. The average width of each domain was estimated to be 1 to 1.5 mm.

The first experiment to be performed on domain walls is to find out the demagnetizing coefficients D_E and induced anisotropy energy K_u along the easy (Z-axis) direction of the sample. These are done by saturating the sample with a d.c. field H_E parallel to the easy and hard axes respectively. Saturation along the easy axis is recognized by the mutual annihilation of the walls, and that along hard axis is recognized by the disappearing of domain contrast. D_E is calculated from $D_E = \mu_0 H_E / M_s \cong 10^{-4}$, where $M_s \cong 0.88T$. This value is not far from the theoretical value¹⁰. Then, K_u is calculated from $H_E = H_K + (D_H M_s) / \mu_0$, where $H_K = 2K_u / M_s$ and D_H is the demagnetizing factor in hard direction. K_u is found to be approximately $3 \times 10^2 J/m^3$.

The second experiment is to take domain wall velocity measurements. They were carried out by applying a pulse field of fixed amplitude to the sample, as shown in Fig. 1 (a). The PG507 pulse generator and TA-1000 power amplifier can produce one pulse or a sequence of pulses with SO-usec pulse lengths. The domain wall positions were observed at the beginning and end of each pulse. Then, wall velocities are determined from the wall displacement Δx and pulse length for each fixed pulse amplitude. These measurements will enable us to find out the wall mobility and other parameters related to the walls. Theoretically speaking, the equation of wall dynamics can be written as, see Fig. 1 (b),

$$m\dot{x} + \beta\dot{x} = 2M_s(H_i - H_c) \quad (1)$$

where m is the effective wall mass per unit area, β is the viscous damping per unit area, and H_i is the internal field. Since the effective wall is small, $m = 1.4 \times 10^{-9} Kg/m^2$ ¹¹, the first term of Eq. (1) is usually neglected. Then, for the internal field,

$$H_i = H_E - \frac{D_E \bar{M}}{\mu_0} \quad (2)$$

where \bar{M} is the average magnetization, which is represented from Fig. 1(b) as

$$\bar{M} = \frac{2\Delta x}{a} M_s \quad (3)$$

Since in each pulse field experiment, $\Delta x/a \cong 10^{-2}$. Then- the demagnetizing field $D_E \bar{M} / \mu_0 \cong 7mOe < H_c < H_E$, where H_c , discussed later, is found to be 20mOe. Hence, from the above argument, the demagnetizing term in Eq. (2) can be neglected for $H_E \geq 100mOe$; and

$H_i \cong H_E$. Eq. (1) is written as

$$\begin{aligned} \beta \dot{x} &= 2M_s(H_E - H_c) \\ V_W = \dot{x} &= \mu(H_E - H_c) \end{aligned} \quad (4)$$

where $\mu = 2M_s/\beta$ is the wall mobility. Eq. (4) is a linear relation between wall velocity V_w and the external field amplitude H_E . This relation is justified from our experimental results, shown in Fig. 2. The slope, which is equal to the wall mobility, is found to be $0.18\text{m}^2/\text{C}$.

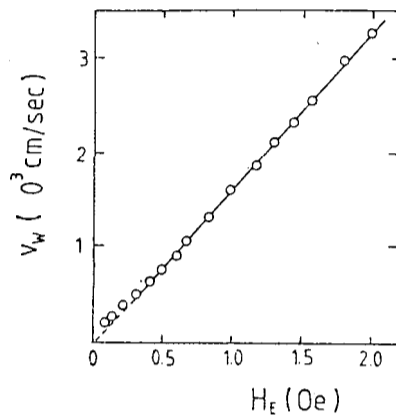


FIG. 2 Wall velocity V_w vs external field H_E in Metglas 2826 MB.

The dotted extrapolation to the H_E - axis is the value of $H_c \cong 17 \text{ mOe}$, which is slightly smaller than the H_c found from the hysteresis measurements discussed later. This is consistent with other measurements."

Since there are usually two kinds of mechanisms responsible for the viscous damping¹², the viscous damping coefficient β is written as

$$\beta = \beta_i + \beta_e \quad (5)$$

β_i is the intrinsic damping coefficient due to spin-relaxation, and β_e is the eddy-current damping coefficient due to the eddy-current. For the case of a rectangular cross-section sample of thickness w , β_i and β_e are expressed as¹²

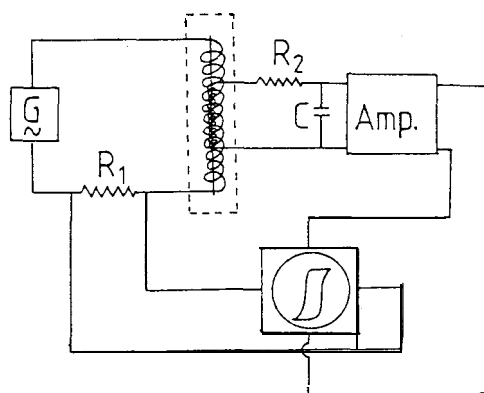
$$\begin{aligned} \beta_e &= (16M_s)^2 w / \pi \rho c^2 \\ \beta_i &= [\alpha(1 + \alpha^2)M_s / \gamma] (K_u / A)^{1/2} \end{aligned} \quad (6)$$

where ρ is the resistivity, c is the speed of light, α is the Gilbert damping from the Landau-Lifshitz equation, $\gamma = 1.76 \times 10^7 \text{ Oe}^{-1}\text{sec}^{-1}$, and A is the exchange stiffness constant. Then, it is straight forward to calculate β_e and from Eqs. (5) and (6), β_i is obtained. Since

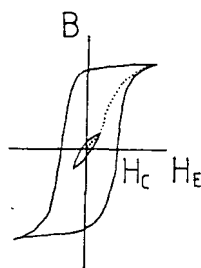
we have measured K_u , and $A \cong 1.0 \times 10^{-11}$ J/m for most of Fe-based alloys, α is calculated to be 0.20. This value agrees with that obtained from a single-crystal Fe whisker sample¹³. Also, from the values of β_i and β_e , we find $\beta_i \cong \beta_e \cong 0$ (10^{-2} Kg/m² sec). This is usually not the case in a crystalline material¹³, where $\beta_i < \beta_e \sim 0$ (1 Kg/m² Sec). The reason for the smaller value of β_e is because of the higher resistivity in amorphous materials.

III. COERCIVITY AND INITIAL PERMEABILITY

A 12 cm long and 2 mm wide strip was cut from the 2826 MB ribbon, and then field annealed in the same manner as described in Sec. II. A hysteresis B-H loop tracer, as shown in Fig. 3(a) was used to measure the coercivity and permeability χ of the material. Because



3(a)



3(b)

FIG. 3(a) The apparatus for the coercivity and permeability measurements.. The dotted line represents the shields to eliminate the earth field.

3(b) The major loop is measured at various frequencies and field amplitudes to obtain H_c and χ . The dotted line is the commutation curve obtained from the minor loops.

of the effect of the earth field, the whole apparatus is well shielded. For the initial magnetization run, the sample was demagnetized. As in Fig. 3(b), H_c is determined for each frequency of the major loop, and the permeability is obtained from the tips of the com-

mutation curve, which is identical to the initial magnetization curve. Then, from these measurements, we can determine the intrinsic properties, such as dc coercivity and initial permeability χ_i (independent of frequency and field amplitude) of the material. From Fig. 4, it is seen that H_c approximately varies as $f^{1/3}$. This is due to the eddy current effect.

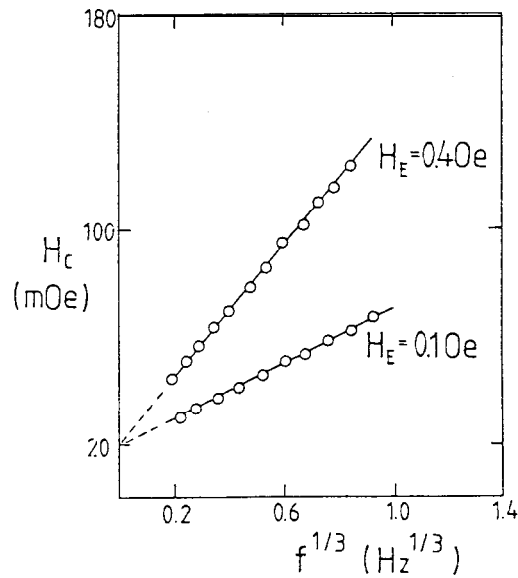


FIG. 4 The coercive force H_c as a function of the external field's frequency f and amplitude H_E .

However, theory has predicted $H_c \propto f^{1/2}$ ¹⁴. The slower frequency dependence probably arises because of breaking into finer domains at high frequency. Our aim here is to find the H_c at the lowest frequency limit, which is approximately 20 mOe. Permeability, is plotted as a function of field amplitude in Fig. 5. The shape of this curve is easily understood from

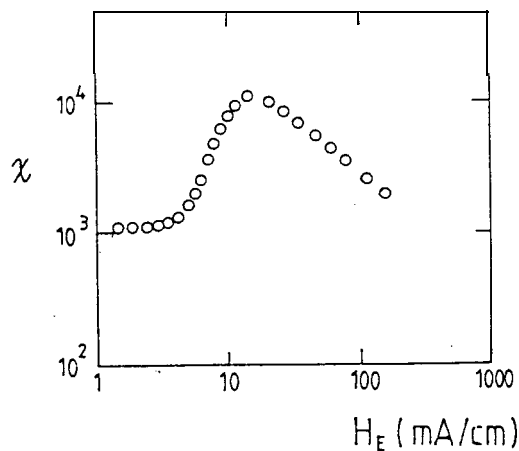


FIG. 5 The permeability measured as a function of field amplitude H_E .

the virgin curve of Fig. 3(b). Then, χ_i is obtained from the low limit of field amplitude,

which is about 10^3 .

Finally, we discuss the relation between H_c and χ_i in the framework of a pinning well model. It is generally observed that for any ferromagnetic material, H_c is almost inversely proportional to χ_i ¹⁵. To understand this phenomenon, we must go to the microscopic picture of any pinning mechanism. In reality, the shapes of pinning wells can be very complex. This is evidenced from the Barkhausen spectrum. However, for simplification, we may approximate the real pinning wells with parabolic wells, as in Fig. 1(c). Mathematically speaking, the pinning force per unit wall area is

$$f_p = \frac{au}{\partial \Delta x} = \frac{2\Delta x}{X_c} M_s \quad (7)$$

where X_c is the size of the well. If a field H_E is applied to move the wall, the equilibrium condition gives,

$$2M_s H_E = f_m = f_p = \frac{2\Delta x}{X_c} M_s \quad (8)$$

Hence

$$\Delta x = \frac{H_E}{H_c} X_c \quad (9)$$

Since two walls move in opposite directions by Δx , the average magnetization \bar{M} is expressed as in Eq. (3). Then, from Eqs. (3) and (9), it is easy to show that

$$\chi_i = \frac{\bar{M}}{\mu_o H_E} = \frac{2X_c M_s}{\mu_o H_c a} \quad (10)$$

Eq. (10) explains the observed relation between χ_i and H_c . With the measured values of χ_i , H_c , M_s and a , we obtain $X_c \cong 1.1 \mu\text{m}$. This is of reasonably correct order of magnitude, because the range of any inhomogeneity, like defects, extends about $1 \mu\text{m}$.

IV. DISCUSSION

We have measured all the important parameters, such as domain width, anisotropy energy, wall mobility and Gilbert damping, concerning a static or dynamic domain wall. Amorphous materials are most suitable for these kinds of measurements with our Kerr-microscopy system. We have also proposed a bulk pinning well model to account for the relation between coercivity and initial permeability. The model is based on the general properties of a domain wall.

REFERENCES

1. R. M. Bozorth, *Ferromagnetism*, (D. Van Nostrand Co., 1951).
2. S. Chikazumi, *Physics of Magnetism* (Wiley, New York, 1964).
3. B. Barbara, J. Magnin and H. Jouve, *Appl. Phys. Lett.* 31, 133 (1977).
4. S. Konishi, T. Hsu and B. R. Brown, *Appl. Phys. Lett.* 30, 497 (1977).
5. R. J. Gambino and T. R. McGuire, *J. Appl. Phys.* 57, 3906 (1985).
6. P. Wolniansky, S. Chase, R. Rosenvold, M. Ruane and M. Mansurpur, *J. Appl. Phys.* 60, 346 (1986).
7. Data Sheets issued by Allied Corporation.
8. D. R. Huang, W. Dow, P. Yao and S. Hsu, *J. Appl. Phys.* 57, 3517 (1985).
9. H. S. Chen, S. D. Ferris, E. M. Gyorgy, H. J. Leamy and R. C. Sherwood, *Appl. Phys. Lett.* 26, 405 (1975).
10. J. A. Osborn, *Phys. Rev.* 57, 351 (1945).
11. A. P. Malozmoff and J. C. Slonczewski, *Magnetic Domain Walls in Bubble Materials*, (Acad. Press, New York, 1979).
12. C. Kittel and J. K. Galt, *Solid State Physics*, Vol. 3 (Acad. Press, 1956).
13. R. W. DeBlois, *J. Appl. Phys.* 29, 459 (1958).
14. E. M. Gyorgy, H. J. Leamy, R. C. Sherwood and H. S. Chen, *AIP Conf. Proc.* 29, 198, 1976.
15. C. Kittel, *Rev. Mod. Phys.* 21, 541 (1949).